CHAPTER 6

X-RAY DIFFRACTION STUDIES OF *x*CuI-(1-*x*)AgI BINARY SYSTEM

Introduction

X-ray diffraction was performed on the materials to determine the effect of CuI on the crystallite size. Peak broadening can also occur as a result of changing crystallite size. Crystallite size can impede or ease ion migration. Hence, it might be possible to understand the variation in the conductivity in the light of crystallite size analyzed through XRD.

6.1 X-Ray Diffraction studies

The room temperature XRD patterns obtained during the present investigation for five different compositions containing pure AgI, 0.1CuI-0.9AgI, 0.2CuI-0.8AgI, 0.3CuI-0.7AgI, and 0.4CuI-0.6AgI are shown in Figure 6.1 to Figure 6.5. X-ray diffraction studies show that pure AgI sintered at 250°C for 5 hours show the presence of β- and γ- phases. This is also reported by Mohan (2004) for pure AgI. Upon addition of CuI (x = 0.1 and x = 0.2), no CuI peaks are observed. (200) peak due to γ-CuI at 2θ = 29.587º is observed in the XRD pattern for x = 0.3 and x = 0.4. The peak increases with CuI content increases.

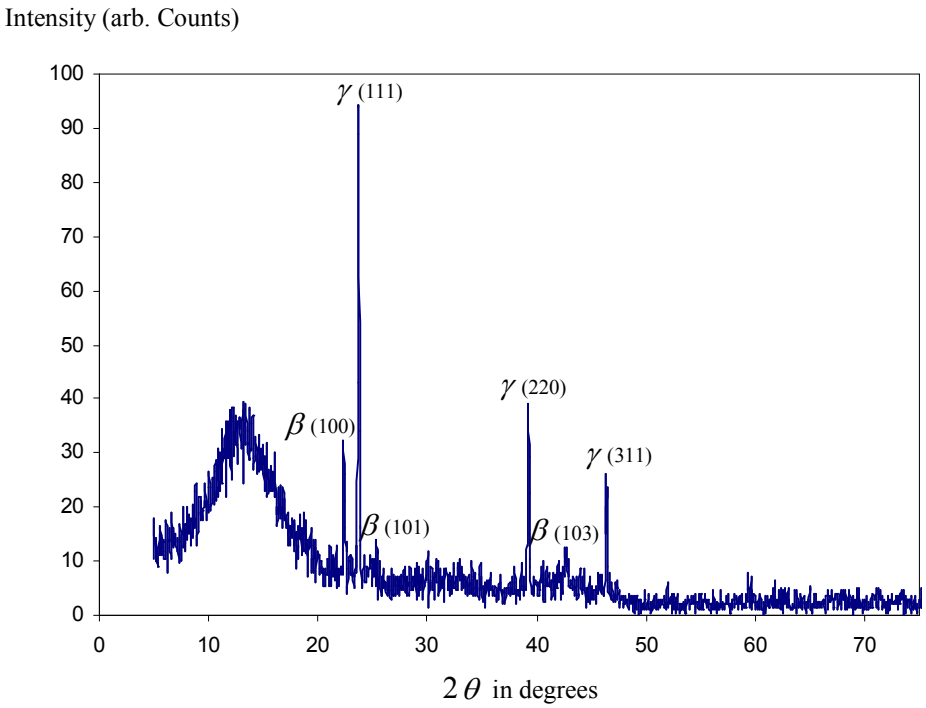

Figure 6.1: X-ray diffraction pattern of pure AgI.

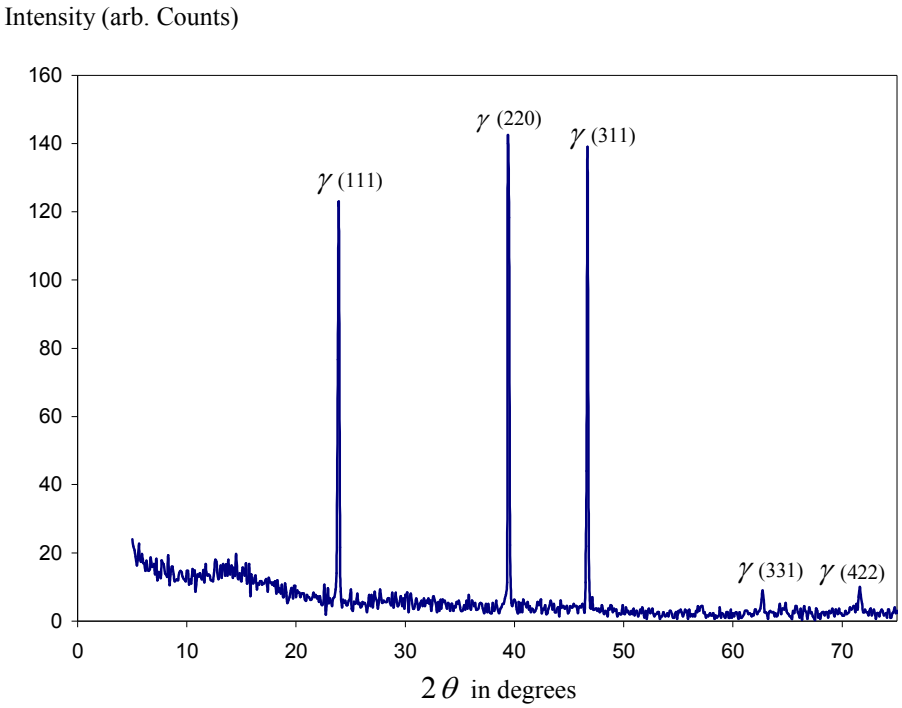

Figure 6.2: X-ray diffraction pattern of 0.1CuI-0.9AgI.

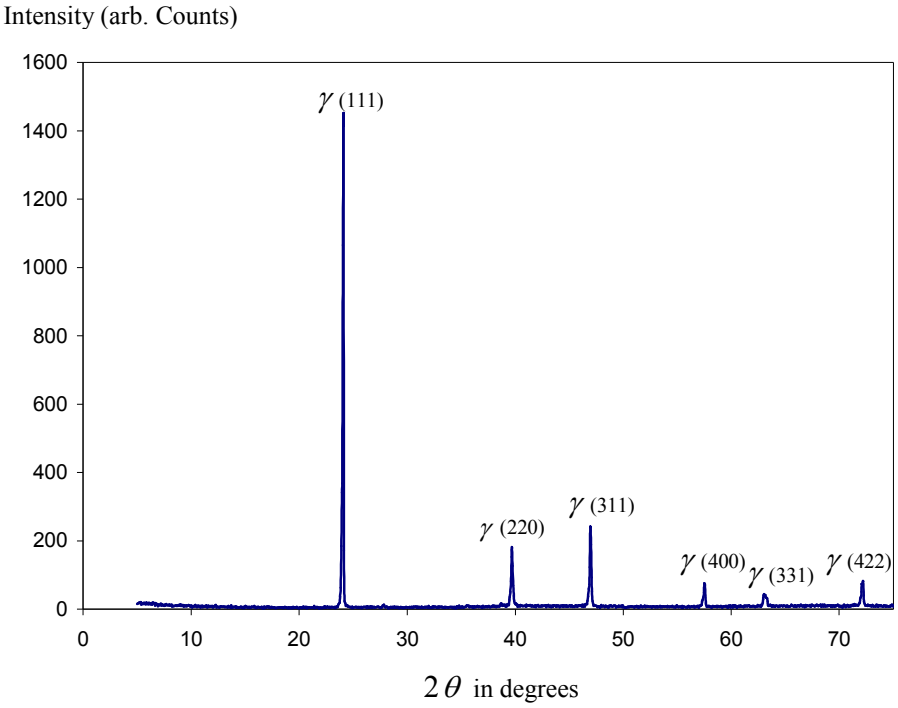

Figure 6.3: X-ray diffraction pattern of 0.2CuI-0.8AgI.

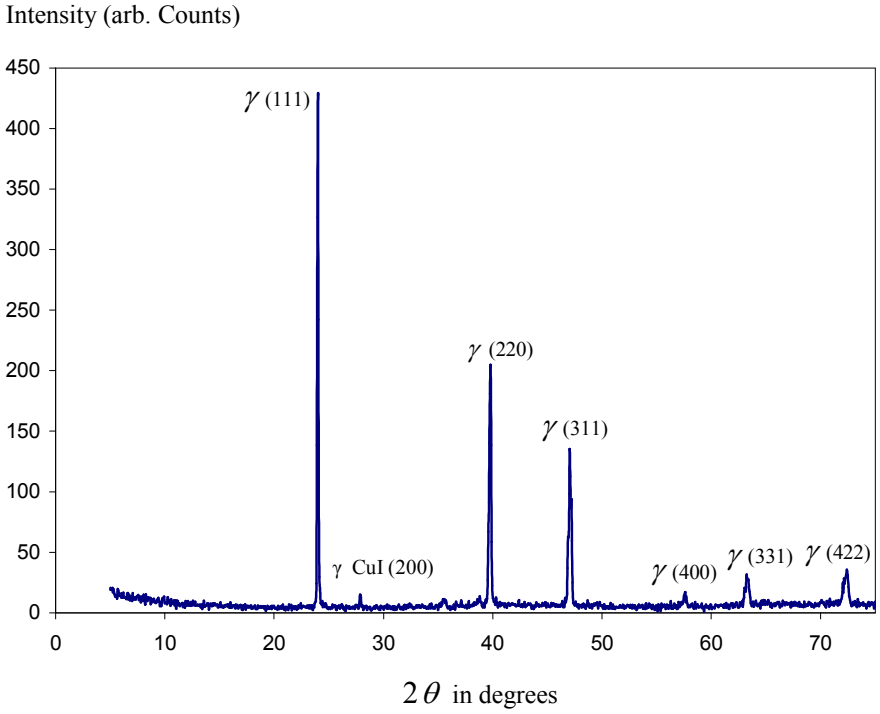

Figure 6.4: X-ray diffraction pattern of 0.3CuI-0.7AgI.

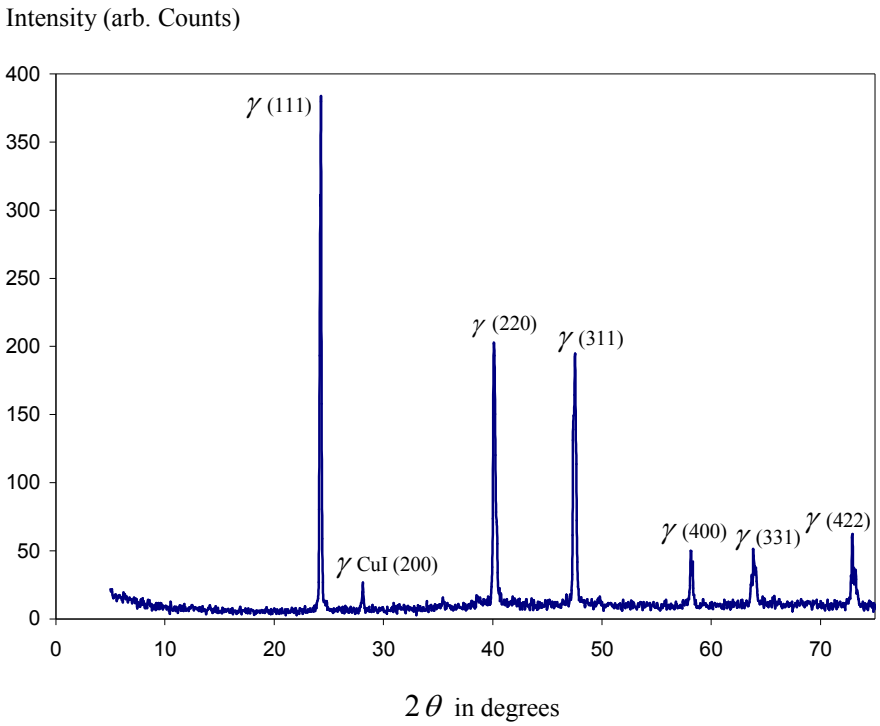

Figure 6.5: X-ray diffraction pattern of 0.4CuI-0.6AgI.

All the XRD patterns presented in the figures are found to show well-defined diffraction lines corresponding. The detection and identification of reflection lines in the XRD patterns have been carried out through the XRD analysis software XRDA aided by JCPDS- International Centre for Diffraction Data.

Undoped AgI reveals the presence of a mixture of two phases which are the major γ-AgI (sphalerite or zincblende structure) and minor β-AgI (wurtzite structure) phase. γ-AgI phase characterized by the XRD peaks at (111), (220) and (311) [a = 649 nm] and β-AgI phase identified by reflections at (100), (101) and (103) [a = 459 nm, c = 751 nm]. It can be seen from Figure 6.1 that the XRD pattern consists of three prominent Bragg peaks which characterized substantial amount of γ-AgI and the presence of additional weak reflections which can be attributed to β-AgI.

The main purpose of Cu doping is to stabilize the metastable- zincblende structure of γ-AgI as well as to assist the reduction of particle size. The Bragg reflections of 0.1CuI-0.9AgI, 0.2CuI-0.8AgI, 0.3CuI-0.7AgI and 0.4CuI-0.6AgI samples show predominant peaks corresponding to only zincblende structure of γ-AgI, meaning that the growth of wurtzite phase of β-AgI is now completely suppressed. This condition suggested a rapid nucleation of γ-AgI crystallites aided by Cu (Mohan, and Sunandana, 2006).

6.2 Crystallite size Analysis

Peak broadening can be attributed to changes in the crystallite size. The graph of D *cos* θ versus 4 *sin* θ can be plotted from which the intersection of the graph at the vertical axis is equal to $0.9\lambda / t$. Here, D represents the broadening of the peak due to the changes in the crystallite size, *t* represents the crystallite size, λ is the wavelength of the X-rays which is 1.5406 Å and θ is the Bragg's angle. Table 6.1 shows the phases of CuI-AgI system and the values of FWHM. Figure 6.6 to Figure 6.10 show the plot of D *cos* θ versus 4 *sin* θ for the binary system.

Table 6.1: Values of FWHM for different phases of xCuI-(1-x)AgI system, ($0 \leq x \leq 0.4$)

x	Phases of xCuI-(1-x)AgI system, ($0 \leq x \leq 0.4$)	FWHM values (°)
0	β (100) γ (111) β(101) γ(220) β(103) γ(311)	0.088 0.120 0.089 0.130 0.190 0.140

Table 6.1: Values of FWHM for different phases of xCuI-(1-x)AgI system, ($0 \leq x \leq 0.4$) (continue)

x	Phases of xCuI-(1-x)AgI system, ($0 \leq x \leq 0.4$)	FWHM values (°)
0.1	γ(111)	0.168
	γ(220)	0.198
	γ(311)	0.129
	γ(331)	0.192
	γ(422)	0.251
0.2	γ(111)	0.104
	γ(220)	0.161
	γ(311)	0.131
	γ(400)	0.157
	γ(331)	0.388
	γ(422)	0.183
0.3	γ(111)	0.139
	γCuI(200)	0.140
	γ(220)	0.203
	γ(311)	0.268
	γ(400)	0.176
	γ(331)	0.313
	γ(422)	0.376
0.4	γ(111)	0.194
	γCuI(200)	0.143
	γ(220)	0.237
	γ(311)	0.331
	γ(400)	0.172
	γ(331)	0.399
	γ(422)	0.116

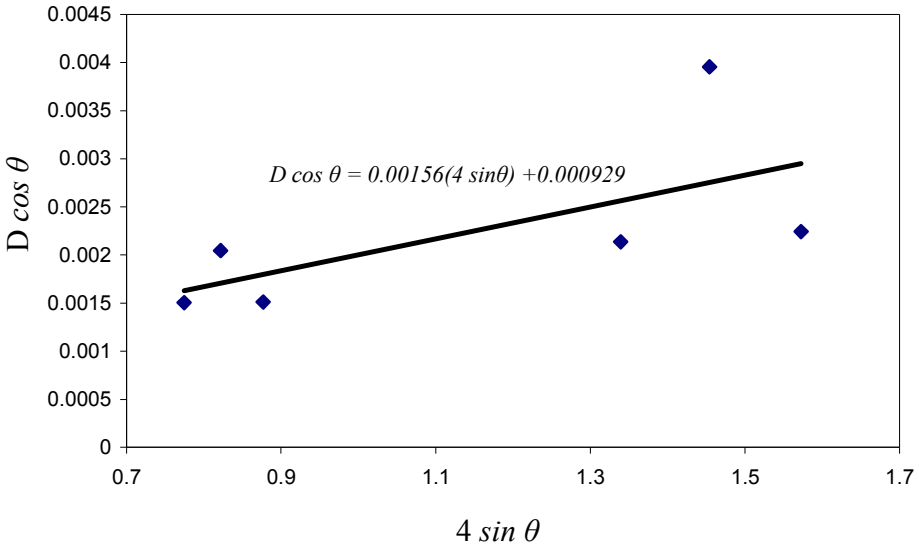

Figure 6.6: Plot of D *cos θ* versus 4 *sin* θ for pure AgI.

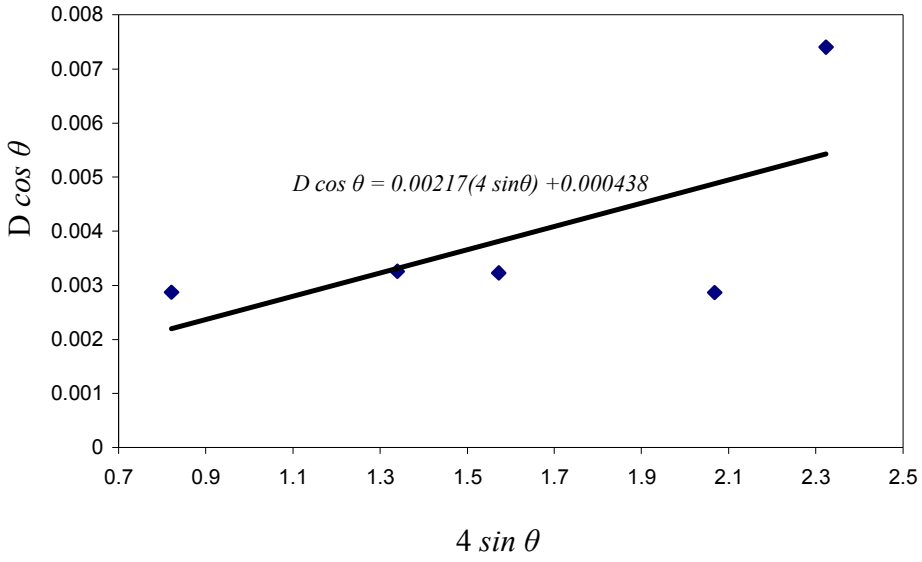

Figure 6.7: Plot of D *cos θ* versus 4 *sin* θ for 0.1CuI-0.9AgI.

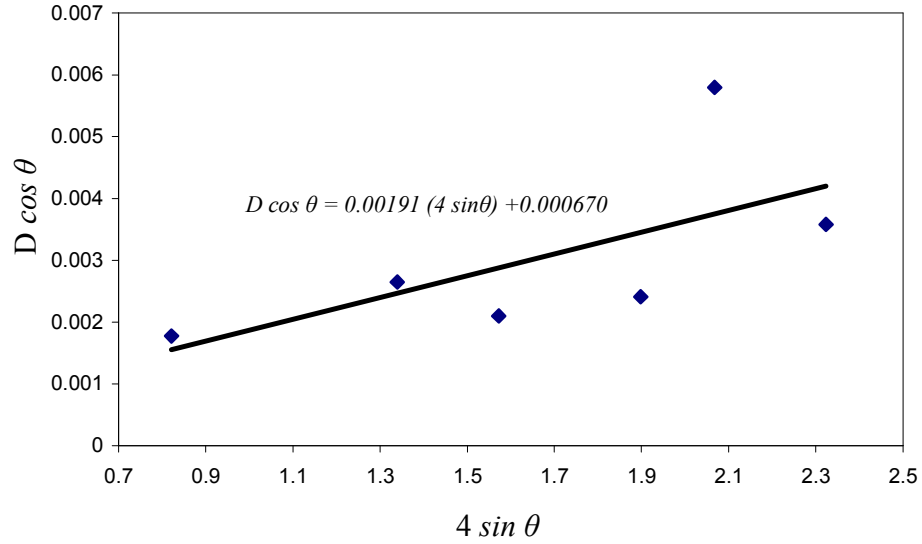

Figure 6.8: Plot of D *cos θ* versus 4 *sin* θ for 0.2CuI-0.8AgI.

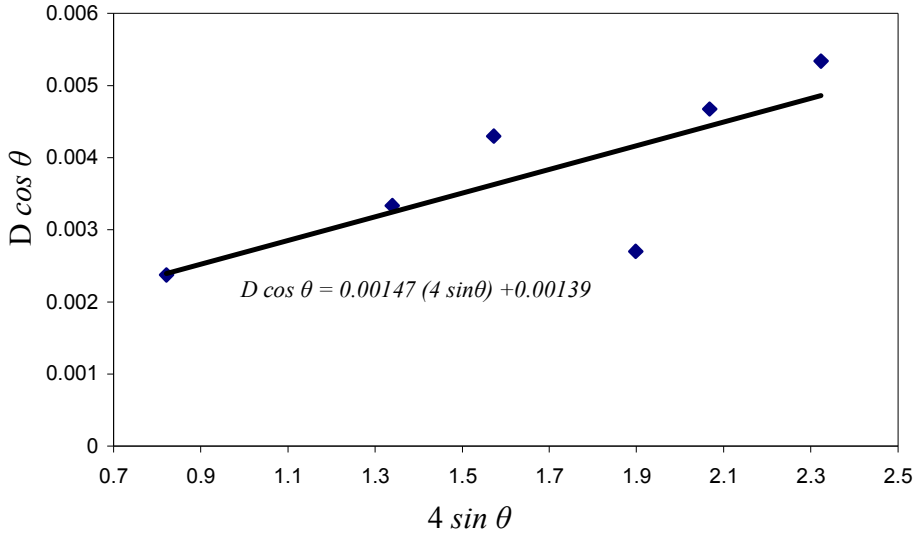

Figure 6.9: Plot of D *cos θ* versus 4 *sin* θ for 0.3CuI-0.7AgI.

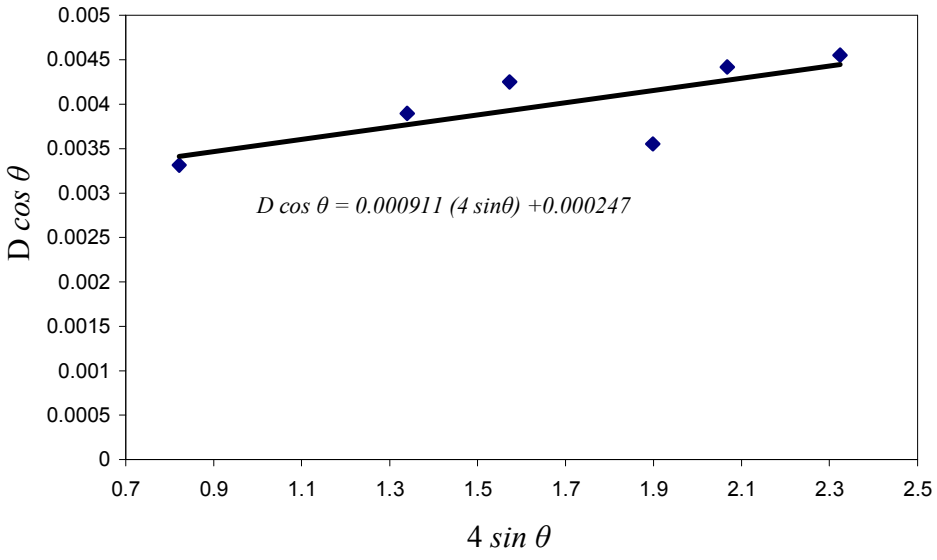

Figure 6.10: Plot of D *cos θ* versus 4 *sin* θ for 0.4CuI-0.6AgI.

Figure 6.11 shows the crystallite size of xCuI-(*1-x)*AgI binary system.

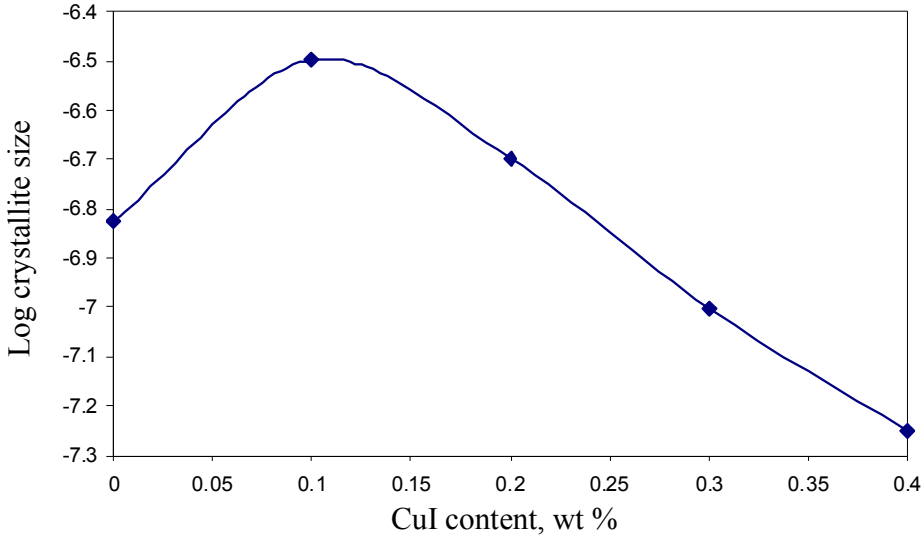

Figure 6.11: Crystallite size of the binary system with various wt % of CuI.

It can be observed from Figure 6.11 that the crystallite size increases when the CuI content in the sample increased.

6.3 Summary

From the XRD pattern, it was found that the substitution of CuI into the *x*CuI-(1-*x*)AgI binary system helped to increase the stability of γ-AgI.